Development of 1-(2-aminophenyl)pyrrole-based amides acting as human topoisomerase I inhibitors

Gabriele Carullo[1,£], Sarah Mazzotta[2,£], Jessica Ceramella[3,£,], Domenico Iacopetta[3], Anna Ramunno[4], Camillo Rosano[5], Antonella Brizzi[6], Giuseppe Campiani[6], Francesca Aiello[3,*] and Maria Stefania Sinicropi[3]

1 Dipartimento di Scienze della Vita, Università degli Studi di Siena, Via Aldo Moro 2, 53100 Siena, Italy
2 Dipartimento di Chimica, Università degli Studi di Milano, Via Golgi 19, 20133 Milano, Italy
3 Dipartimento di Farmacia e Scienze della Salute e della Nutrizione, Università della Calabria, Edificio Polifunzionale 87036 Rende (CS), Italy
4 Dipartimento di Farmacia, Università degli Studi di Salerno, Via Giovanni Paolo II 132, 84084, Fisciano (SA), Italy.
5 Unità di Proteomica e Spettrometria di Massa, IRCCS Ospedale Policlinico San Martino, Largo Rosanna Benzi 10, 16132 Genova, Italy.
6 Dipartimento di Biotecnologie, Chimica e Farmacia, Università degli Studi di Siena, Via Aldo Moro 2, 53100 Siena, Italy.

£these authors contributed equally
*Correspondence: Prof. Francesca Aiello, Department of Pharmacy, Health and Nutritional Science, University of Calabria, Edificio Polifunzionale 87036 Rende (CS), Italy. Email: francesca.aiello@unical.it

Abstract
Topoisomerases are ubiquitous enzymes in the human body, particularly involved in cancer development and progression. Topoisomerase I (topoI) performs DNA relaxation reactions by "controlled rotation" rather than by "strand passage". The inhibition of topoI has become a useful strategy to control cancer cell proliferation. Nowadays, different compounds underwent clinical trials, but the search for new molecular entities is necessary and benefits from medicinal chemistry efforts. Pyrrole-based compounds emerged as promising anti-proliferative agents, with particular interest in breast cancer therapy and topoI inhibition. Starting from these observations and based on the scaffold-hopping approach, we developed a small library of 1-(2-aminophenyl)pyrrole-based amides (**7a-f**) as new anti-cancer agents. Tested on a panel of cancer cell lines, **7a-f** displayed the most interesting profile in MDA-MB-231 cells, where the most active compounds, **7d-f**, were able to induce death by apoptosis. Direct enzymatic assays and docking simulations on the topoI active site (PDB: 1A35) revealed the inhibitory activity and potential binding site for the newly developed 1-(2-aminophenyl)pyrrole-based amides.

KEYWORDS 1-(2-aminophenyl)pyrrole, topoIB inhibitors, apoptosis, breast cancer, anti-proliferative, docking simulation.

1 INTRODUCTION

The International Agency for Research on Cancer estimated that by 2030 cancer deaths worldwide will surpass 13 million per year due to the growth and ageing of the population. Chemotherapeutics play a key role in this context, but the validation of new targets and the development of more potent drugs is necessary[1]. DNA topoisomerases, known as the 'cellular magicians'[2] are ubiquitous enzymes that regulate nucleic acid strands' topology, especially DNA, and all the genome functions. In particular, their functions consist of the relaxation of DNA by freeing the torsional strain, due to supercoiling, and change in DNA topology by breaking and re-joining double-stranded DNA, by a nucleophile attacking at the phosphodiester backbone. DNA topoisomerases are classified into type I and II based on their structures and catalytic activity. Type I topoisomerases (topoI) cut one of the strands of double-stranded DNA, and are classified in three subtypes: IA, IB, and IC, which are present in different organisms. TopoIB, expressed in eukaryotic cells, cleaves a single DNA strand through its Tyr723 residue and generates a phosphotyrosine linkage to the DNA. Consequentially, the fragmented DNA strand is able to rotate around the unbroken strand and eliminate DNA supercoiling. In fact, topoIB performs DNA relaxation reactions by "controlled rotation" rather than by "strand passage".[3] TopoIB is often over-expressed in several tumor cells. The inhibition of topoIB has become a useful strategy to control cancer cell proliferation and interference with the function of topoIB by small molecules in different types of cancers, in combination therapy or not, is an important area of research. Generally, topoI inhibitors include poisons, as camptothecin and derivatives that covalently trap topoI on DNA (cleavage complex formation), or catalytic ones, which prevent DNA cleavage, as carbazole or phenanthridine derivatives.[4–7] Numerous are topoI poisons under clinical trials.[8] Few topo-modulators have been already marketed, such as topotecan and irinotecan, analogues of alkaloid camptothecin **1** (**Figure 1**), that despite widely used, suffer severe drawbacks (bone marrow suppression, hair loss, breathlessness, high fever, and vomiting, drug-related leukemia and drug-resistance) [9,10]. **1** is a natural alkaloid isolated from extracts of *Camptotheca acuminata*, selective topoI poison and displayed robust antineoplastic action against colorectal, breast, lung and ovarian cancers[11]. In the structure of **1** there are several fused heterocycles, one of them containing a lactone function, which seems to be relevant for the inhibitory activity, and nitrogen-based rings such as quinolines, which showed an interesting inhibition profile versus topoI enzymes. Nitrogen heterocycles, opportunely decorated, displayed a wide panel of biological activities[12–14], including anticancer efficacy [15,16]. Pyrrole-based small molecules such as obatoclax **2**, sunitinib **3**, and ulixertinib **4** (Figure 1) showed promising anticancer effects.[17] This scaffold has also been encountered in known topoisomerase inhibitors [18] and is sometimes decorated by an amide group [19]. Among the privileged scaffolds[20–22], also indole and quinoline have been used in the past for the development of topoisomerase inhibitors. The natural alkaloid ellipticine **5** and the synthetic quinoline compound **6** (**Figure 1**) showed good inhibitory properties against topoIB[7,23,24], fostering the development of new interesting topoIB inhibitors, namely pyrroloquinolines [11,25]. The pharmacophore model, common to anti-topoisomerase agents, is constituted by a planar aromatic scaffold, that promotes the DNA intercalation, and a hydrogen bond donor side chain, that favors contact with the enzyme[25]. Based on our interest in developing breast cancer inhibitors[26], exemplified by 7-substituted 5*H*-pyrrole [1,2-*a*][3,1]benzoxazin-5-one derivatives[27], and [1,2-*a*]-pyrroloquinoxaline derivatives [28–30], and having topoIB as the biological target, our efforts were addressed to generate by a "scaffold hopping" approach new 1-(2-aminophenyl)pyrrole-based amides (**Figure 1**) [31]. We developed a small series of *N*-(1*H*-pyrrol-1-yl) phenyl amides **7a**-**f** by merging phenylpyrrole structure with different heterocycles (indole, quinoline,

pyridine, pyrazine), embedded through an amide bond (**Figure 1**). In this context, a one-pot protocol was used (**Scheme 1**) involving acyl donor and 1-(2-aminophenyl)pyrrole as starting materials in Steglich conditions, avoiding extra-steps and employing cheap reagents under mild conditions. These compounds were designed with the aim to have only the essential pharmacophoric elements useful for topoIB inhibition. The synthesized compounds **7a-f** were firstly evaluated for their ability to induce anti-cancer effects in different cell lines, including ER+ and triple-negative breast (MCF-7 and MDA-MB-231 respectively), neuroblastoma (SH-SY5Y) and melanoma (A2508) cancer cells, without affecting normal cell viability. The ability to interact with topoIB was evaluated by means of the *in vitro* relaxation assay. TUNEL assay was employed to confirm the apoptosis of the most interesting compounds in MDA-MB-231 cells, while docking analyses on the active site of topoIB (PDB:1A35) were performed to investigate the binding mode of selected compounds.

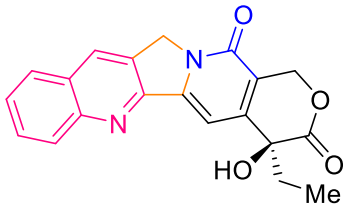

1

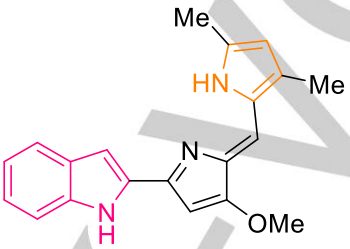

2

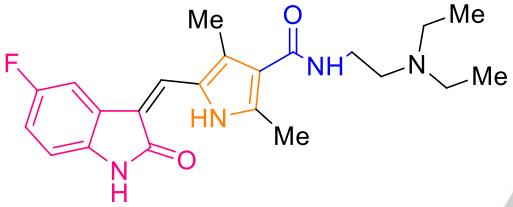

3

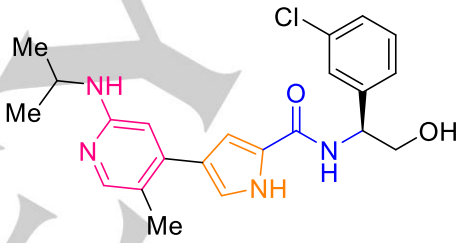

4

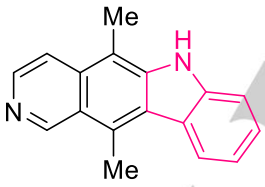

5

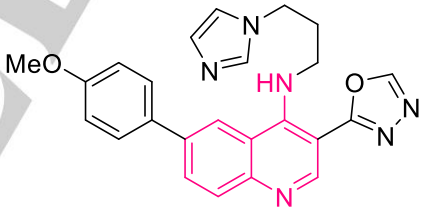

6

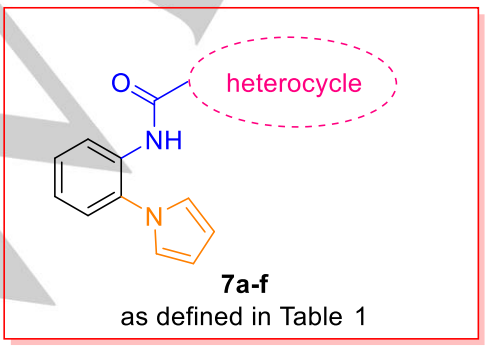

7a-f
as defined in Table 1

Figure 1. Reference topoI inhibitors and general structure of the novel compounds **7a-f**

2 RESULTS AND DISCUSSION

2.1 Chemistry

The synthesis of target compounds **7a**-**f** was performed starting from commercially available low-cost reagents as described in **Scheme 1**. In particular, 2-amino phenylpyrrole **8** was reacted with different carboxylic acids **9a**-**f** under Steglich conditions, in presence of EDCI/HOBt couple as activating agent in dry dichloromethane as solvent.

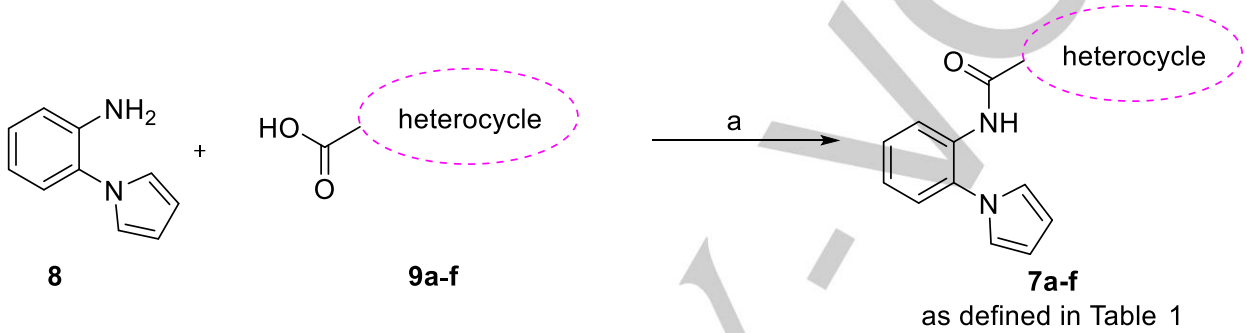

SCHEME 1. Synthesis of compounds **7a-f**. Reagents and conditions: a) EDCI, HOBt, dry DCM, from 0 to 25 °C, 72 h.

2.2 *Anti-cancer activity of 7a-f and SAR analysis*

The compounds **7a**-**f** synthesized here are characterized by a general pattern, simplified in the 2-aminophenylpyrrole moiety, in which the aniline moiety has been variously decorated by using acyl donors able to form amide bonds. In this context, the "scaffold hopping" approach was used to obtain new topoIB inhibitors, characterized by the essential nitrogen moieties useful to obtain the best performing inhibitors. The biological evaluation of **7a**-**f** has been performed *via* 3-(4,5-dimethylthiazol-2-y1)-2,5-diphenyltetrazolium (MTT) analysis in cancer and non-cancerous cells (**Tables 1,2**). The anti-cancer ability of all synthesized compounds was evaluated toward two breast cancer cell lines, namely the ER+ MCF-7 and triple-negative MDA-MB-231 cells, the melanoma A2058 and the human epithelial neuroblastoma SHSY-5Y cells. As reported in **Table 1**, all the compounds resulted more active against the breast cancer cells, mostly towards the highly aggressive and metastatic MDA-MB-231 cells. MCF-7 cell line was less sensitive than MDA-MB-231 cells to all the tested compounds, indeed the best compounds able to decrease the viability of MCF-7 cells, **7a** and **7b**, possessed IC_{50} values of 1.21±0.1 and 0.79±0.2 µM, respectively. The other compounds showed higher IC_{50} values, ranging from 2.14±0.9 to 4.36±0.8 µM. A lower anticancer activity was found against the neuroblastoma SHSY-5Y and melanoma A2058 cells, where **7f** resulted the most active compound with IC_{50} values of 53.92±0.7 and 21.95±0.9 µM, respectively. Moreover, compounds **7d** and **7e** reduced, as well, the growth of the melanoma A2058 cells with IC_{50} values of 60.74±1.1 and 55.69±1.0 µM, respectively, while compound **7c** was also active towards the neuroblastoma cells with an IC_{50} value of 73.29±1.0 µM. The other compounds showed IC_{50} values higher than 100 µM against both the melanoma and neuroblastoma cells. MDA-MB-231 cells resulted to be highly sensitive to these compounds. In fact, a good anti-cancer activity was recorded under the exposure of compounds **7a-c**, showing IC_{50} values very close each other, *i.e.* 0.59±0.1, 0.58±0.1 and 0.55±0.1 µM, respectively, suggesting that the presence of pyrazine or

pyridine moieties do not alter significantly the anti-cancer activity. On the other hand, compounds **7d-f**, which are decorated with bulkier chemical groups at the amide function, resulted the most active, showing IC_{50} values of 0.27±0.1, 0.48±0.1 and 0.47±0.1µM against the MDA-MB-231 cells, respectively (**Table 1**). Moreover, all compounds were also tested against two normal cells, namely the human mammary epithelial MCF-10A cells and the mouse embryonic fibroblasts BALB/3T3, in order to investigate the selectivity of all the tested compounds on cancer cells (**Table 2**). All the compounds resulted non-cytotoxic against both the normal cells used in this assay, at least until the concentration of 100 µM and under the adopted experimental conditions. Compound **5** was used as reference molecule. As shown in **Table 1,** it has a better anti-cancer activity than our derivatives in all the cancer cells used except for the MDA-MB-231, where our derivatives resulted more active, and compound **7b** in MCF-7 cells (**Table 1**).

Table 1. Anti-cancer activity of the studied compounds expressed as IC_{50} values ± S.D. µM, against different cell lines.

	Chemical Structure	Cell line			
		MCF-7	**MDA-MB-231**	**SH-SY5Y**	**A2058**
7a	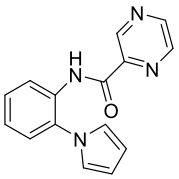	**1.21±1.0**	**0.59±0.1**	**>100**	**>100**
7b	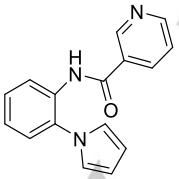	**0.79±0.2**	**0.58±0.1**	**>100**	**>100**
7c	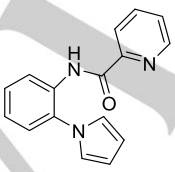	**2.14±0.9**	**0.55±0.1**	**73.29±1.0**	**>100**

7d	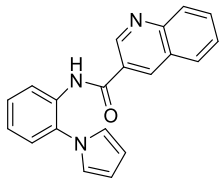	**2.28±0.7**	**0.27±0.1**	**>100**	**60.74±1.1**
7e	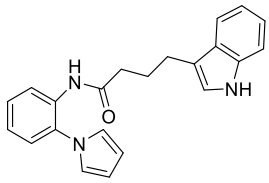	**4.36±0.8**	**0.48±0.1**	**>100**	**55.69±1.0**
7f	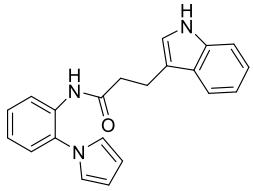	**2.90±1.1**	**0.47±0.1**	**53.92±0.7**	**21.95±0.9**
5		**1.28±1.0**	**1.77±0.9**	**1.85±1.1**	**1.57±1.3**

However, **5** is characterized by a high toxicity on normal cells (IC_{50} values= 1.31±0.8 and 1.02±0.2 on MCF-10A and BALB/3T3 cells, respectively) when compared with all the developed compounds (**Table 2**).

Table 2. Cytotoxicity evaluation of the studied compounds on normal cells, expressed as IC_{50} values ± S.D. µM.

	Compounds						
Cell line	**7a**	**7b**	**7c**	**7d**	**7e**	**7f**	**5**
BALB-3T3	>100	>100	>100	>100	>100	>100	1.31±0.8
MCF-10A	>100	>100	>100	>100	>100	>100	1.02±0.2

2.3 Relaxation of supercoiled DNA: Validation of compounds as human topoI inhibitors

Numerous literature data reported the ability of some pyrrole carboxamide derivatives to interfere with DNA-dependent enzymes, for example topoisomerases [32]. Among these enzymes, topoI induces transient DNA single-strand breaks, thus regulating the level of the double helix supercoiling[33] and recent studies have identified this enzyme as an important therapeutic target in cancer therapy[34]. Compounds able to interfere with this enzyme are very useful in targeted therapies and may produce therapeutic benefits for many cancer types, including breast [35]. Starting from these considerations, we determined the capability of the most interesting compounds in terms of anti-cancer activity, **7d-f**, to interfere with the human topoI activity, performing an *in vitro* relaxation assay. In particular, we incubated the substrate (supercoiled plasmid pHOT1) with the enzyme and the selected compounds or vehicle (see Material and methods for more details). **Figure 2** depicts the obtained results, where is evident the ability of all the used compounds to inhibit the topo I activity, with some differences. Indeed, among the three tested compounds, **7e** showed to be the best topoI inhibitor, as it was able to totally inhibit the activity of this enzyme at 10 µM **(Figure 2, lane 6)** but, more interestingly, as well at the concentration of 1 µM **(Figure 2, lane 5)**. Certainly, the presence of a single band of DNA at the bottom of the agarose gel corresponds to the supercoiled DNA, indicating the lack of the topoI activity. A different behaviour was found when the enzyme was incubated in the presence of compound **7d**. The latter was able to inhibit the topoI activity only partially and with a dose-dependent behaviour (1 and 10 µM). In fact, together with a slighter band of the supercoiled plasmid in the lower part of the gel, multiple bands corresponding to the relaxed products of the DNA are also noticeable **(Figure 2, lanes 3 and 4,** 1 and 10 µM, respectively**)**. Finally, compound **7f** was found to be a less potent inhibitor, when compared to the other two compounds. Indeed, **7f** did not inhibit the enzyme activity at the concentration of 1 µM, as indicated by the presence of multiple bands (relaxed DNA products, **Figure 2, lane 7)**, similar to those visible in the control reaction **(Figure 2, lane 2)**. Raising the concentration to 10 µM, only a feeble inhibitory activity was detected, indicated by the presence of a slight band of supercoiled DNA in the lower part of the gel **(Figure 2, lane 8)**. These outcomes suggest that the difference of a methylene unit between **7e** and **7f** (butanamide *vs* propanammide) strongly influenced the topo I inhibitory activity. To sum up, **7e** totally inhibited the topo I activity already at the concentration of 1 µM whereas, compounds **7d** and **7f** are weaker inhibitors.

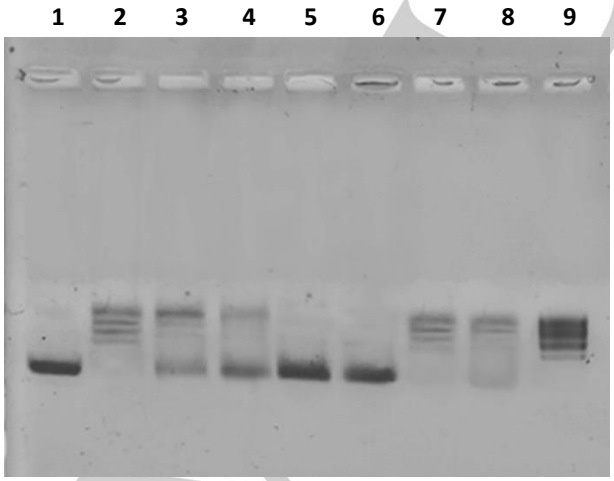

Figure 2. Human topo I relaxation assay. topoI was incubated with the vehicle alone (CTRL) or with the tested compounds used at 1 and 10 µM, using the supercoiled (SC) DNA pHOT1 as substrate. Lane 1, SC pHOT1; lane 2, CTRL (DMSO); lanes 3 and 4, **7d** at

1 and 10 µM, respectively; lanes 5 and 6, **7e** at 1 and 10 µM, respectively; lanes 7 and 8, **7f** at 1 and 10 µM, respectively; lane 9, relaxed DNA marker. The figure is representative of three independent experiments.

2.4 Molecular docking analysis on human topoIB

Molecular docking was adopted to better understand the possible binding modes of the compounds described above **(Figure 1, Tables 1,2)** with topoI (PDB: 1A35). We used a "blind-docking approach" for our simulations: this kind of procedure has been successfully used by our research group in several other studies[36,37]. With these simulations, we aimed at one side to identify the most promising candidate among the three most active compounds and, on the other side, to improve the atomic structure of the molecules to design and synthesize better lead compounds. We calculated the compound binding affinities to the topoI using the program Autodock (Autodock is a tool that calculates a binding affinity constant K_i based on the binding energy between the protein and its ligand, according to the expression K_i = exp (deltaG/ (R*T)). To rank the possible binding modes, we took into consideration the clusterization of the results from the simulations, as discussed in previous works[37–41]. Binding energies for the three compounds are reported in **Table 3**.

Table 3. Binding energies and affinities of the different compounds to topoI

Compound	Binding Energy (Kcal/mol)	K_i (µM)
7d	-8.97	0.26
7e	-7.65	2.46
7f	-7.73	2.14

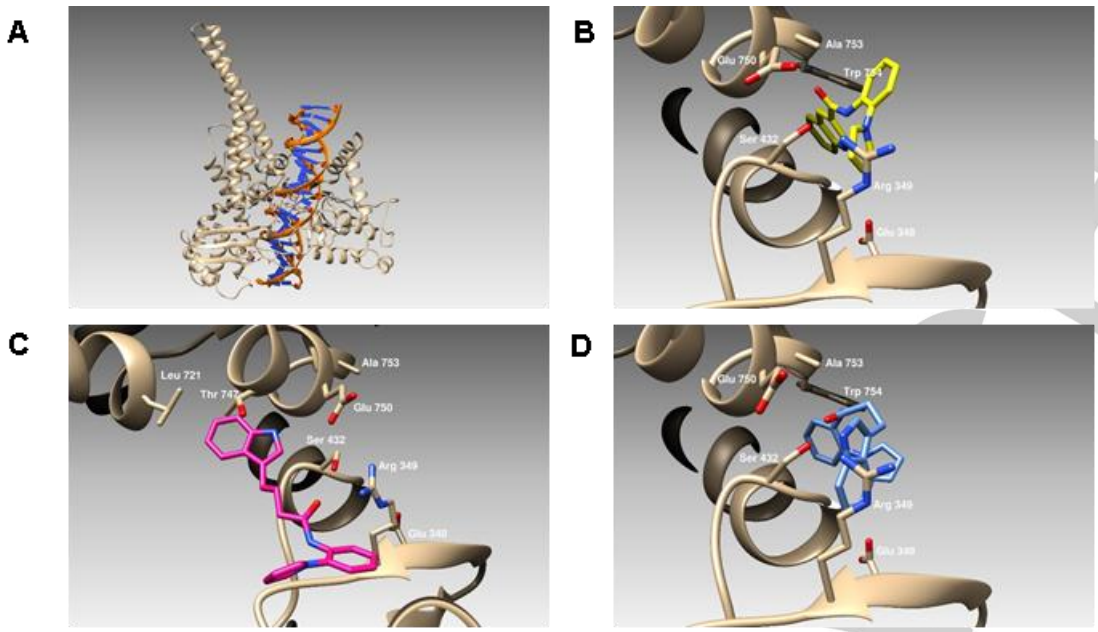

Figure 3. The three-dimensional structure of the topoI bound to DNA **(Panel A)** and compounds **7d (panel B), 7e (panel C)** and **7f (panel D)**. Proteins are schematically reported as ribbons. Ligands binding poses are described as colored sticks.

Finally, the obtained best poses for each compound were visually examined to evaluate the quality of the protein-ligand interactions. The obtained simulations suggested that our compounds were able to dock the topoI forming hydrogen bonds and hydrophobic interactions. A possible binding site for the compounds lies in the proximity of the protein-DNA binding zone **(Figure 3, panel A).** Compound **7d** binds topoI establishing hydrogen bonds with Arg349, Ser432 and Glu750 and hydrophobic interactions with the side chains of residues Glu348, Arg434, Trp441, and Ala 753. Furthermore, compound **7d** participates in π-π stacking interactions with the indole moiety of Trp754 **(Figure 3, panel B)**. In the same pose, compound **7f** f **(Figure 3, panel D)**. Compound **7e (Figure 3, panel C)** lays on the opposite site with respect of Ser 432 and forms hydrogen bonds with Arg 349, Ser432 and Thr747 residues. The ligand is further stabilized by hydrophobic interactions with residues Ile335, Pro431, and Leu721.

2.4 *7d-f targeting topoI showed proapoptotic effect: TUNEL assay*

The inhibition of the topoI activity provokes the DNA damage and its failure to be repaired could triggers cancer cell death by apoptosis[42]. For these reasons, we investigated the capability of compounds **7d-f** to induce apoptosis in MDA-MB-231 breast cancer cells by means of a specific *in vitro* test, the TUNEL assay. Our outcomes clearly showed that MDA-MB-231 cells treated with **7d-f**, at their IC_{50} values for 24 hours, underwent massive apoptosis, as evidenced by a strong green nuclear fluorescence that indicates the formation of fragmented/damaged DNA (**Figure 4, panels B**, compounds **7d, 7e** and **7f**). Contrarily, in the control experiment conducted on MDA-MB-231 cells exposed only to the vehicle (DMSO), no green nuclear fluorescence was detected, indicating the lack of any DNA damage (**Figure 4, panel B**, CTRL).

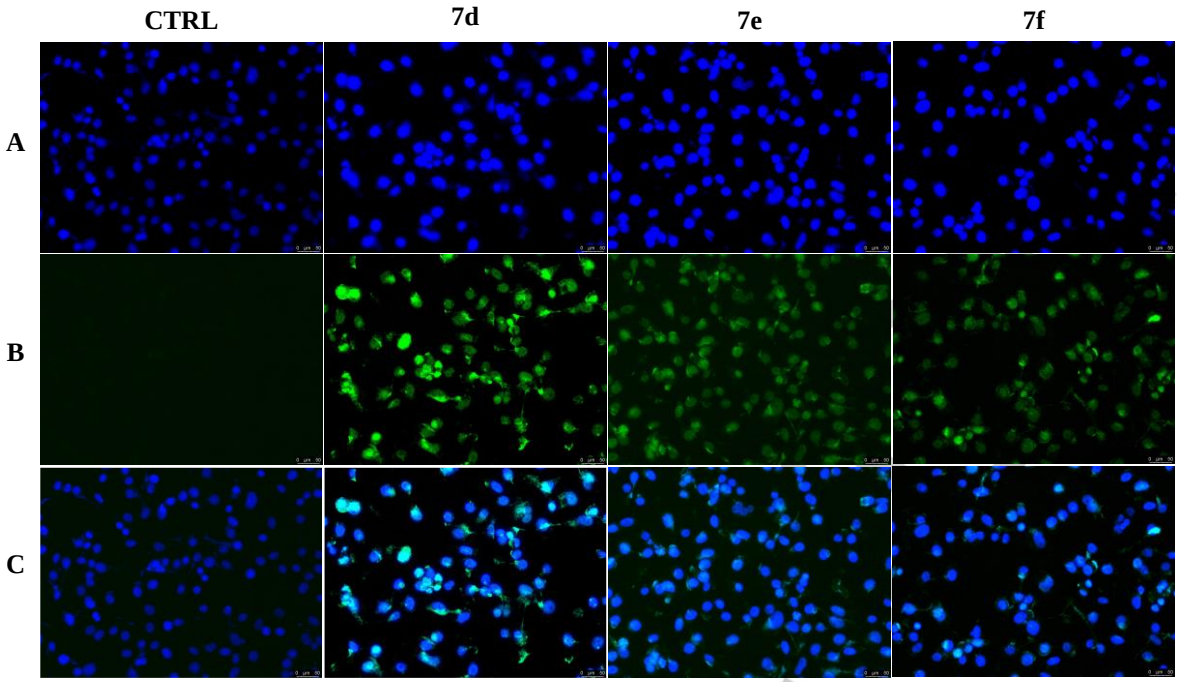

Figure 4. TUNEL assay. MDA-MB-231 cells were treated with compounds **7d-f** at their IC_{50} values or with vehicle (CTRL) for 24 h. Then, cells were processed and imaged under an inverted fluorescence microscope (20x magnification). Panels A: DAPI ($\lambda_{ex}/\lambda_{em}$ = 350/460 nm); Panels B: CF^{TM}488A ($\lambda_{ex}/\lambda_{em}$ = 490/515 nm) Panels C: overlay channels. Fields represent three different experiments.

3 CONCLUSION

In this work, new topoI inhibitors based on pyrrole scaffold were developed. By using the scaffold-hopping approach, 1-(2-aminophenyl)pyrrole-based amides **7a-f** were synthesized and validated as anti-cancer agents in different cell lines. **7a-f** showed interesting anti-cancer properties, especially in MDA-MB-231 triple-negative breast cancer cells. **7a-f** did not show cytotoxic effects in normal BALB/3T3 and MCF-10A cells. *In vitro* topoI inhibition assays for selected compounds **7d-f** showed interesting profiles at the concentration of 1 and 10 µM. Docking simulations on the topoI active site revealed that the potential binding mode for **7d,f** is similar, while compound **7e** lays on the opposite site of the groove. Considering that topoI inhibition mediates apoptosis induction, we performed a TUNEL assay in order to confirm the cell death mechanism for **7d-f** in MDA-MB-231 cells.

4 EXPERIMENTAL

4.1 Chemistry

4.1.1 General

All the reagents were purchased from Merck (Darmstadt, Germany) or Alfa Aesar (Tewksbury, MA, USA) and were used as received. Melting points were obtained using a Gallenkamp (G) (Fiorano Modenese, Italy) melting point apparatus. The structures of final compounds were unambiguously assessed by ^{1}H NMR (nuclear magnetic resonance) and ^{13}CNMR. Spectra were recorded in the indicated solvent (Chloroform-$CDCl_3$, Acetone-d_6) at 25 °C on a Bruker 300 MHz spectrometer (Bruker, Milano, Italy) employing TMS

(tetramethyl silane) as internal standard. Chemical shifts are expressed in values (ppm) and coupling constants (*J*) in hertz (Hz). Reactions were monitored by TLC (thin layer chromatography) on silica gel plates Merck 60 F254 (Merck, Burlington, MA, USA). Final products were purified by a flash chromatography system with column chromatography, using Merck 60 silica gel, 230–400 mesh. Elemental analyses were performed on Leco Trunspec CHNS Micro elemental system (St. Joseph, MI, USA). ESI-HRMS spectra were acquired by a linear ion-trap-Orbitrap hybrid mass spectrometer (LTQOrbitrap XL) (Thermo Fisher Scientific, Bremen, Germany) operating in positive electrospray ionization mode. Data were collected and analyzed using the Xcalibur 2.2 software provided by the manufacturer. The purity of the final compounds was evaluated by C, H, N analysis, and it was confirmed to be ≥ 95%.

4.1.2 General procedure for the synthesis of compounds 7a-f

1-(2-Aminophenyl)pyrrole (1.82 mmol, 1.2 eq) and the corresponding carboxylic acid (1.6 mmol, 1.0 eq) were dissolved in dry DCM (5 mL) under N_2 and cooled to 0 °C, then *N*-hydroxybenzotriazole (HOBt) (1.92 mmol, 1.2 eq) was added and the reaction was stirred for 15 min. After this time, 1-ethyl-3-(3-dimethylaminopropyl) carbodiimide (EDCI) (1.92 mmol, 1.2 eq) was dissolved in dry DCM (3 mL) and added dropwise to the mixture. The whole reaction mixture was stirred at room temperature until TLC showed the full conversion (72 h), and then it was concentrated under reduced pressure. The crude was dissolved in ethyl acetate and washed with 5% $NaHCO_3$ solution (x2), NH_4Cl (x2) and brine. The organic phase was dried over Na_2SO_4, filtered and concentrated to dryness. The crude product was further purified by flash chromatography (SiO_2) using petroleum ether/ethyl acetate as eluent in an appropriate ratio.

N-[2-(1H-Pyrrol-1-yl)phenyl]pyrazine-2-carboxamide (7a)

The product was purified by flash chromatography (petroleum ether/ethyl acetate 3:1). Yellow solid. Y = 37%. mp = 132-133 °C. HRMS ESI *m/z* $[M+Na]^+$ calcd for $[C_{15}H_{12}ON_4Na]^+$ 287.0903, found 287.0902. Anal. Calcd for $C_{15}H_{12}N_4O$: C, 68.17; H, 4.58; N, 21.20. Found: C, 68.21; H, 4.60; N, 21.25. ^{1}H NMR (300 MHz, Acetone-d_6) δ 9.82 (s, 1H), 9.30 (s, 1H), 8.83 (s, 1H), 8.63-8.52 (m, 2H), 7.47 (t, *J* = 6.0 Hz, 1H), 7.37 (d, *J* = 6.2 Hz, 1H), 7.29-7.23 (m, 1H), 6.97 (s, 2H), 6.35 (s, 2H). ^{13}C NMR (75 MHz, $CDCl_3$) δ ^{13}C NMR (75 MHz, $CDCl_3$) δ 161.0, 147.5, 144.5, 144.2, 142.6, 132.9, 131.3, 128.7, 127.0, 124.8, 122.1, 121.1, 110.4.

N-[2-(1H-Ppyrrol-1-yl)phenyl]nicotinamide(7b)

The product was purified by flash chromatography (petroleum ether/ethyl acetate 3:1). Yellow oil. Y = 43%. HRMS ESI *m/z* $[M+H]^+$ calcd for $[C_{16}H_{14}ON_3]^+$ 264.1131, found 264.1118. Anal. Calcd for $C_{16}H_{13}N_3O$: C, 72.99; H, 4.98; N, 15.96. Found: C, 73.02; H, 4.98; N, 16.00. ^{1}H NMR (300 MHz, $CDCl_3$) δ 8.74 (s, 1H), 8.53 (d, *J* = 8.2 Hz, 1H), 7.99 (s, 1H), 7.82 (s, 1H), 7.59 – 7.07 (m, 4H), 6.84 (s, 2H), 6.45 (s, 2H). ^{13}C NMR (75 MHz, $CDCl_3$) δ 163.0, 157.2, 133.7, 131.2, 129.1, 126.9, 126.8, 124.8, 122.2, 121.4, 121.3, 110.9, 110.8.

N-[2-(1H-Pyrrol-1-yl)phenyl]picolinamide (7c)

The product was purified by flash chromatography (petroleum ether/ethyl acetate 3:1). White solid. Y = 50%. mp = 117 °C. HRMS ESI *m/z* $[M+H]^+$ calcd for $[C_{16}H_{14}ON_3]^+$ 264.1131, found 264.1127. Anal. Calcd for $C_{16}H_{13}N_3O$: C, 72.99; H, 4.98; N, 15.96. Found: C, 73.04; H, 5.01; N, 15.97. ^{1}H NMR (300 MHz, $CDCl_3$) δ 8.67 (d, *J* = 8.2 Hz, 1H), 8.46 (d, *J* = 5.0 Hz, 1H), 8.23 (d, *J* = 8.2 Hz, 1H), 7.84 (ddd, *J* = 8.8 Hz, *J* = 7.1 Hz, *J* = 1.5 Hz, 1H), 7.46-

7.36 (m, 2H), 7.33 (dd, *J* = 8.2 Hz, *J* = 1.4, Hz, 1H), 7.17 (ddd, *J* = 8.6 Hz, *J* = 7.5 Hz, *J* = 1.6 Hz, 1H), 6.88 (t, *J* = 2.2 Hz, 2H), 6.42 (t *J* = 2.1 Hz, 2H). ^{13}C NMR (75 MHz, $CDCl_3$) δ 163.2, 149.8, 147.2, 138.3, 136.6, 133.5, 132.2, 129.4, 127.8, 123.1, 121.6, 121.2, 111.2, 109.1.

N-[2-(1H-Pyrrol-1-yl)phenyl]quinoline-3-carboxamide (7d)

The product was purified by crystallization with ethanol. White crystals. Y = 33%. mp = 157 ° C. HRMS ESI *m/z* $[M+H]^+$ calcd for $[C_{20}H_{16}ON_3]^+$ 314.1288, found 314.1293; *m/z* $[M+Na]^+$ calcd for $[C_{20}H_{15}ON_3Na]^+$ 336.1107, found 336.1115. Anal. Calcd for $C_{20}H_{15}N_3O$: C, 76.66; H, 4.83; N, 13.41. Found: C, 76.64; H, 4.88; N, 13.40. ^{1}H NMR (300 MHz, Acetone-d_6) δ 8.31 (d, *J* = 2.3 Hz, 1H), 8.18 (s, 1H), 7.79 – 7.74 (m, 1H), 7.19 (dd, *J* = 13.8 Hz, *J* = 8.3 Hz, 2H), 7.12 – 7.05 (m, 1H), 6.94 (ddd, *J* = 8.5 Hz, *J* = 6.9 Hz, *J* = 1.5 Hz, 1H), 6.75 (ddd, *J* = 8.1 Hz, *J* = 6.9 Hz, *J* = 1.2 Hz, 1H), 6.58 – 6.42 (m, 3H), 6.10 (t, *J* = 2.1 Hz, 2H), 5.38 (t, *J* = 2.1 Hz, 2H). ^{13}C NMR (75 MHz, Acetone-d_6) δ 163.9, 149.3, 148.6, 135.6, 134.3, 132.8, 131.3, 129.1, 129.0, 127.7, 127.4, 127.3, 126.7, 126.4, 126.0, 125.3, 121.9, 109.9.

N-[2-(1H-Pyrrol-1-yl)phenyl]-4-(1H-indol-3-yl)butanamide (7e)

The product was purified by flash chromatography (petroleum ether/ethyl acetate 2:1). Beige solid. Y = 55%. mp = 142 ° C. HRMS ESI *m/z* $[M+Na]^+$ calcd for $[C_{22}H_{21}ON_3Na]^+$ 366.1577, found 366.1578. Anal. Calcd for $C_{22}H_{21}N_3O$: C, 76.94; H, 6.16; N, 12.24. Found: C, 76.98; H, 6.12; N, 12.24. ^{1}H NMR (300 MHz, $CDCl_3$) δ 8.42 (d, *J* = 8.2 Hz, 1H), 7.96 (s, 1H), 7.59 (d, *J* = 7.8 Hz, 1H), 7.47 – 7.32 (m, 2H), 7.31 – 7.05 (m, 4H), 7.00 (s, 1H), 6.97 – 6.88 (m, 1H), 6.77 (t, *J* = 2.1 Hz, 2H), 6.38 (t, *J* = 2.1 Hz, 2H), 2.81 (t, *J* = 7.3 Hz, 2H), 2.29 (t, *J* = 7.4 Hz, 2H), 2.20 – 1.83 (m, 2H). ^{13}C NMR (75 MHz, $CDCl_3$) δ 174.5, 138.0, 129.1, 126.7, 123.8 (2C), 122.1 (4C), 121.8, 119.2, 118.6, 111.3, 110.2 (4C), 25.5, 24.1.

N-[2-(1H-Pyrrol-1-yl)phenyl]-3-(1H-indol-3-yl)propenamide (7f)

The product was purified by flash chromatography (petroleum ether/ethyl acetate 2:1). Beige solid. Y = 40%. mp = 155 ° C. HRMS ESI *m/z* $[M+H]^+$ calcd for $[C_{21}H_{20}ON_3]^+$ 330.1601, found 330.1608; *m/z* $[M+Na]^+$ calcd for $[C_{21}H_{19}ON_3Na]^+$ 352.1420, found 352.1423. Anal. Calcd for $C_{21}H_{19}N_3O$: C, 76.57; H, 5.81; N, 12.76. Found: C, 76.60; H, 5.84; N, 12.77. ^{1}H NMR (300 MHz, $CDCl_3$) δ 8.34 (d, *J* = 8.1 Hz, 1H), 8.09 (s, 1H), 7.53 (d, *J* = 7.7 Hz, 1H), 7.33 (dd, *J* = 12.5, 4.8 Hz, 2H), 7.25 – 6.93 (m, 4H), 6.87 (d, *J* = 2.3 Hz, 1H), 6.81 (s, 1H), 6.50 (t, *J* = 2.1 Hz, 2H), 6.20 (t, *J* = 2.1 Hz, 2H), 3.08 (t, *J* = 7.3 Hz, 2H), 2.58 (t, *J* = 7.3 Hz, 2H). ^{13}C NMR (75 MHz, $CDCl_3$) δ 171.9, 128.7 (2C), 126.7 (2C), 124.0 (2C), 122.0 (3C), 121.4, 119.2, 118.9 (2C), 111.1, 110.4, 37.1, 25.4, 24.3.

4.2 Biological assays

4.2.1 Cell Cultures

The use cell lines (breast cancer cells MCF-7 and MDA-MB-231, melanoma cells A2058 and human mammary epithelial cells MCF-10A) were obtained from American Type Culture Collection (ATCC, Manassas, VA, USA) and cultured as already indicated [43]. The human epithelial neuroblastoma cells SHSY-5Y and the mouse embryonic fibroblasts BALB/3T3 were also purchased from American Type Culture Collection (ATCC, Manassas, VA, USA) and cultured in DMEM high glucose supplemented with 100 U mL^{-1} penicillin/streptomycin and 10% fetal bovine serum (FBS) and bovine calf serum (BCS), respectively.

4.2.2 MTT Assay

MTT assays [Sigma Aldrich (St. Louis, MO, USA)] were used to determine the *in vitro* anticancer activities of all the studied compounds, following an already reported protocol[44]. The compounds were tested at different concentrations (0.01-0.1-1-10-25-50-100 μM) for 72 h and the IC_{50} values were calculated from the percent (%) of control using GraphPad Prism 9 (GraphPad Software, La Jolla, CA, USA).

4.2.3 Human topol Relaxation Assay

The topoI relaxation assays were performed incubating supercoiled pHOT1, used as substrate, with the recombinant topoI (TopoGEN, Port Orange, FL, USA) and compounds, as indicated in the manufacturer's protocol (TopoGEN, Port Orange, FL, USA), with some modifications [45]. Briefly, topo I relaxation assays were performed in a final volume of 20 µL, in which 0.25 µg of supercoiled pHOT1 was added to a solution containing the tested compounds. The mix was incubated for 15 min at 37 ◦C. Then, the reaction was initiated by addition of recombinant topoI (2 U), incubated at 37 ◦C for 1 h and terminated by the addition of 5× stop buffer. The obtained solution was loaded onto a 1% agarose gel containing 1× TAE buffer without ethidium bromide (EB). At the end, 1× TAE buffer containing EB (0.5 µg/mL) was used to stain agarose gel for 30 min and after washing with distilled water for 15 min, it was visualized using a UV transilluminator.

4.2.4 TUNEL assay

TUNEL assay was performed to determine the cells' apoptosis, following the manufacturer's protocols (CF™488A TUNEL Assay Apoptosis Detection Kit, Biotium, Hayward, CA, USA), with few revisions as previously described[46]. DAPI (0.2 µg/mL, Sigma Aldrich, Milan, Italy) was used for nuclei staining and the fluorescence detection was performed using a fluorescence microscope (Leica DM 6000, 20x magnification). LAS-X software allowed to acquire and process all the images, which are representative of three separate experiments.

4.3 Molecular docking

The three-dimensional models of topoI was built using as a template the crystal structures of the topoI in covalent and noncovalent complexes with DNA (PDB code 1A35) as previously described [44]. The three-dimensional structures of the tested compounds were built and energy minimized using the program MarvinSketch [ChemAxon ltd, Budapest, Hu]. In order to evaluate the possible binding modes of the three compounds to the topoI and calculate their binding energies, we used the program suite Autodock v.4.2.2 [41]. Following the protocol adopted in several other experiences [37–40], we adopted a "blind docking" strategy for our simulations: the docking of the compounds to topoI have been done without any *a priori* knowledge of the binding site by the system. We performed all the simulations adopting the standard program default values. The protein and the ligands were prepared using the abstract data type graphical interface[14,47]. To reduce the computational time, we considered the ligands as fully flexible objects, while the protein target has been considered as fully rigid. A cluster analysis was performed based on root mean squares deviation (RMSD) values of each pose with respect to the starting geometry. The lowest energetic conformation of the most populated cluster was considered as the best candidate. In case two or more clusters were almost equipopulated and their energy distribution is spread, the corresponding were considered as bad ligands [48]. The docking poses resulting from our simulations were ranked in order of their binding energy values and clustered on the basis of a RMSD cut-off value of 2.0 Å. From the structural analysis of the lowest energy solutions of each cluster, we could spot the putative protein binding site. Figure 3 has been drawn using the program Chimera [49].

CONFLICT OF INTEREST

The authors declare no conflict of interest

REFERENCES

[1] F. Bray, J. Ferlay, I. Soerjomataram, R. L. Siegel, L. A. Torre, A. Jemal, *CA Cancer J Clin* **2018**, *68*, 394–424.

[2] M. Kadagathur, S. Patra, G. Devabattula, J. George, R. Phanindranath, A. S. Shaikh, D. K. Sigalapalli, C. Godugu, N. Nagesh, N. D. Tangellamudi, N. Shankaraiah, *Eur J Med Chem* **2022**, *238*, 114465.

[3] F. You, C. Gao, *Curr Top Med Chem* **2019**, *19*, 713–729.

[4] M. A. Cinelli, *Med Res Rev* **2019**, *39*, 1294–1337.

[5] Y. Pommier, *Nature Reviews Cancer 2006 6:10* **2006**, *6*, 789–802.

[6] G. Aichinger, F.-B. Lichtenberger, T. N. Steinhauer, I. Flörkemeier, G. Del Favero, B. Clement, D. Marko, *Molecules* **2020**, *25*, 25071524.

[7] J. Ceramella, D. Iacopetta, A. Caruso, A. Mariconda, A. Petrou, A. Geronikaki, C. Rosano, C. Saturnino, A. Catalano, P. Longo, M. S. Sinicropi, *Pharmaceuticals* **2023**, *16*, 353.

[8] J. Y. Jang, D. Kim, N. D. Kim, *International Journal of Molecular Sciences* **2023**, *24*, 8457.

[9] M. Fuertes, A. Selas, A. Trejo, B. R. Knudsen, F. Palacios, C. Alonso, *Bioorg Med Chem Lett* **2022**, *57*, 128517.

[10] A. Thomas, Y. Pommier, *Clinical Cancer Research* **2019**, *25*, 6581–6589.
[11] A. Mazza, E. M. Beccalli, A. Contini, A. N. Garcia-Argaez, L. Dalla Via, M. L. Gelmi, *Eur J Med Chem* **2016**, *124*, 326–339.
[12] S. Gemma, G. Campiani, S. Butini, G. Kukreja, B. P. Joshi, M. Persico, B. Catalanotti, E. Novellino, E. Fattorusso, V. Nacci, L. Savini, D. Taramelli, N. Basilico, G. Morace, V. Yardley, C. Fattorusso, *J Med Chem* **2007**, *50*, 595–598.
[13] E. Morelli, S. Gemma, R. Budriesi, G. Campiani, E. Novellino, C. Fattorusso, B. Catalanotti, S. S. Coccone, S. Ros, G. Borrelli, V. Kumar, M. Persico, I. Fiorini, V. Nacci, P. Ioan, A. Chiarini, M. Hamon, A. Cagnotto, T. Mennini, C. Fracasso, M. Colovic, S. Caccia, S. Butini, *J Med Chem* **2009**, *52*, 3548–3562.
[14] A. Frandsen, D. S. Pickering, B. Vestergaard, C. Kasper, B. B. Nielsen, J. R. Greenwood, G. Campiani, C. Fattorusso, M. Gajhede, A. Schousboe, J. S. Kastrup, *Mol Pharmacol* **2005**, *67*, 703–713.
[15] C. Fattorusso, S. Gemma, S. Butini, P. Huleatt, B. Catalanotti, M. Persico, M. De Angelis, I. Fiorini, V. Nacci, A. Ramunno, M. Rodriquez, G. Greco, E. Novellino, A. Bergamini, S. Marini, M. Coletta, G. Maga, S. Spadari, G. Campiani, *J Med Chem* **2005**, *48*, 7153–7165.
[16] G. Campiani, T. Khan, C. Ulivieri, L. Staiano, C. Papulino, S. Magnano, S. Nathwani, A. Ramunno, D. Lucena-Agell, N. Relitti, S. Federico, L. Pozzetti, G. Carullo, A. Casagni, S. Brogi, F. Vanni, P. Galatello, M. Ghanim, N. McCabe, S. Lamponi, M. Valoti, O. Ibrahim, J. O'Sullivan, R. Turkington, V. P. Kelly, R. VanWemmel, J. F. Díaz, S. Gemma, D. Zisterer, L. Altucci, A. De Matteis, S. Butini, R. Benedetti, *Eur J Med Chem* **2022**, *235*, 114274.
[17] B. Żołnowska, J. Sławiński, Z. Brzozowski, A. Kawiak, M. Belka, J. Zielińska, T. Baczek, J. Chojnacki, *Int J Mol Sci* **2018**, *19*, 1482.
[18] J. Kovvuri, B. Nagaraju, V. L. Nayak, R. Akunuri, M. P. N. Rao, A. Ajitha, N. Nagesh, A. Kamal, *Eur J Med Chem* **2018**, *143*, 1563–1577.
[19] A. S. Tikhomirov, V. A. Litvinova, D. V. Andreeva, V. B. Tsvetkov, L. G. Dezhenkova, Y. L. Volodina, D. N. Kaluzhny, I. D. Treshalin, D. Schols, A. A. Ramonova, M. M. Moisenovich, A. A. Shtil, A. E. Shchekotikhin, *Eur J Med Chem* **2020**, *199*, 112294.
[20] M. Badolato, G. Carullo, M. C. Caroleo, E. Cione, F. Aiello, F. Manetti, *ACS Med Chem Lett* **2019**, *10*, 402–406.
[21] G. Carullo, L. Bottoni, S. Pasquini, A. Papa, C. Contri, S. Brogi, V. Calderone, M. Orlandini, S. Gemma, K. Varani, S. Butini, F. Galvagni, F. Vincenzi, G. Campiani, *ChemMedChem* **2022**, *17*, e202200456.
[22] S. Mazzotta, L. Frattaruolo, M. Brindisi, C. Ulivieri, F. Vanni, A. Brizzi, G. Carullo, A. R. Cappello, F. Aiello, *Future Med Chem* **2019**, *12*, 5–17.
[23] A. Talukdar, B. Kundu, D. Sarkar, S. Goon, M. A. Mondal, *Eur J Med Chem* **2022**, *236*, 114304.
[24] P. Rizza, M. Pellegrino, A. Caruso, D. Iacopetta, M. S. Sinicropi, S. Rault, J. C. Lancelot, H. El-Kashef, A. Lesnard, C. Rochais, P. Dallemagne, C. Saturnino, F. Giordano, S. Catalano, S. Andò, *Eur J Med Chem* **2016**, *107*, 275–287.
[25] L. Dalla Via, G. Marzaro, A. Ferrarese, O. Gia, A. Chilin, *Eur J Med Chem* **2014**, *77*, 103–109.
[26] M. Badolato, G. Carullo, F. Aiello, A. Garofalo, *J Chem* **2017**, *2017*, 2370359.
[27] M. Badolato, G. Carullo, B. Armentano, S. Panza, R. Malivindi, F. Aiello, *Bioorg Med Chem Lett* **2017**, *27*, 3092–3095.
[28] F. Aiello, G. Carullo, F. Giordano, E. Spina, A. Nigro, A. Garofalo, S. Tassini, G. Costantino, P. Vincetti, A. Bruno, M. Radi, *ChemMedChem* **2017**, *12*, 1279–1285.
[29] G. Carullo, S. Mazzotta, F. Giordano, F. Aiello, *J Chem* **2021**, *2021*, 5596816.
[30] M. Perri, F. Aiello, E. Cione, G. Carullo, L. Amendola, S. Mazzotta, M. C. Caroleo, *Front Mol Biosci* **2019**, *6*, article 12.
[31] S. Zheng, Z. Lei, H. Ai, H. Chen, D. Deng, Y. Yang, *J Cheminform* **2021**, *13*, 87.

[32] M. H. David-Cordonnier, M. P. Hildebrand, B. Baldeyrou, A. Lansiaux, C. Keuser, K. Benzschawel, T. Lemster, U. Pindur, *Eur J Med Chem* **2007**, *42*, 752–771.
[33] Y. Pommier, *Nature Reviews Cancer* **2006**, *6*, 789–802.
[34] J. L. Delgado, C. M. Hsieh, N. L. Chan, H. Hiasa, *Biochem J* **2018**, *475*, 373–398.
[35] T. Baudino, *Curr Drug Discov Technol* **2015**, *12*, 3–20.
[36] M. R. Redinbo, L. Stewart, P. Kuhn, J. J. Champoux, W. G. J. Hol, *Science* **1998**, *279*, 1504–1513.
[37] C. Rosano, M. Ponassi, M. F. Santolla, A. Pisano, L. Felli, A. Vivacqua, M. Maggiolini, R. Lappano, *AAPS Journal* **2016**, *18*, 41–46.
[38] M. S. Sinicropi, D. Iacopetta, C. Rosano, R. Randino, A. Caruso, C. Saturnino, N. Muià, J. Ceramella, F. Puoci, M. Rodriquez, P. Longo, M. R. Plutino, *J Enz Inhib Med Chem* **2018**, *33*, 434–444.
[39] N. Abbassi, E. M. Rakib, H. Chicha, L. Bouissane, A. Hannioui, C. Aiello, R. Gangemi, P. Castagnola, C. Rosano, M. Viale, *Arch Pharm* **2014**, *347*, 423–431.
[40] M. F. Santolla, E. M. De Francesco, R. Lappano, C. Rosano, S. Abonante, M. Maggiolini, *Cell Signal* **2014**, *26*, 1466–1475.
[41] G. M. Morris, H. Ruth, W. Lindstrom, M. F. Sanner, R. K. Belew, D. S. Goodsell, A. J. Olson, *J Comput Chem* **2009**, *30*, 2785–2791.
[42] O. Sordet, Q. A. Khan, K. W. Kohn, Y. Pommier, *Curr Med Chem Anticancer Agents* **2003**, *3*, 271–290.
[43] J. Ceramella, C. La Torre, M. De Luca, D. Iacopetta, A. Fazio, A. Catalano, G. Ragno, P. Longo, M. S. Sinicropi, C. Rosano, *PeerJ* **2022**, *10*, e13683.
[44] D. Iacopetta, A. Mariconda, C. Saturnino, A. Caruso, G. Palma, J. Ceramella, N. Muià, M. Perri, M. S. Sinicropi, M. C. Caroleo, P. Longo, *ChemMedChem* **2017**, *12*, 2054–2065.
[45] D. Iacopetta, C. Rosano, F. Puoci, O. I. Parisi, C. Saturnino, A. Caruso, P. Longo, J. Ceramella, A. Malzert-Fréon, P. Dallemagne, S. Rault, M. S. Sinicropi, *Eur J Pharm Sci* **2017**, *96*, 263–272.
[46] D. Iacopetta, A. Carocci, M. S. Sinicropi, A. Catalano, G. Lentini, J. Ceramella, R. Curcio, M. C. Caroleo, *ChemMedChem* **2017**, *12*, 381–389.
[47] "PSB - Abstract," can be found under http://psb.stanford.edu/psb-online/proceedings/psb99/abstracts/p401.html, **n.d.**
[48] C. Rosano, R. Lappano, M. F. Santolla, M. Ponassi, A. Donadini, M. Maggiolini, *Curr Med Chem* **2015**, *19*, 6199–6206.
[49] E. F. Pettersen, T. D. Goddard, C. C. Huang, G. S. Couch, D. M. Greenblatt, E. C. Meng, T. E. Ferrin, *J Comput Chem* **2004**, *25*, 1605–1612.

Entry for the Table of Contents

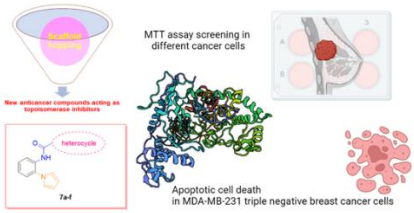

1-(2-aminophenyl)pyrrole-based amides promote apoptosis *via* topoisomerase I inhibition